THE ASTROPHYSICAL JOURNAL, 601:L13–L16, 2004 January 20

A CHARACTERISTIC DENSE ENVIRONMENT OR WIND SIGNATURE IN PROMPT GAMMA-RAY BURST AFTERGLOWS

SHIHO KOBAYASHI,[1,2] PETER MÉSZÁROS,[1,2,3] AND BING ZHANG[1]
Received 2003 August 22; accepted 2003 December 1; published 2004 January 9

ABSTRACT

We discuss the effects of synchrotron self-absorption in the prompt emission from the reverse shock of gamma-ray burst afterglows in a dense environment, such as the wind of a stellar progenitor or a dense interstellar medium in early galaxies. We point out that when synchrotron losses dominate over inverse Compton losses, the higher self-absorption frequency in a dense environment implies a bump in the reverse-shock emission spectrum, which can result in a more complex optical/IR light curve than previously thought. This bump is prominent especially if the burst ejecta is highly magnetized. In the opposite case of low magnetization, inverse Compton losses lead to a prompt X-ray flare. These effects give a possible new diagnostic for the magnetic energy density in the fireball and for the presence of a dense environment.

Subject headings: gamma rays: bursts — radiation mechanisms: thermal — shock waves

1. INTRODUCTION

Snapshot fits of the broadband spectrum of gamma-ray burst (GRB) afterglows to forward-shock models have been found, in many cases, to be consistent with an external environment density $n \lesssim 1$ cm^{-3} typical of a diluted interstellar medium (ISM) that can be taken to be approximately independent of distance from the burst (Frail et al. 2001). In other cases, the forward shock is better fitted with an external density that depends on distance as $\rho \propto R^{-2}$, typical of a stellar wind environment (Chevalier & Li 1999, 2000; Li & Chevalier 2003). The two types of fits have been critically analyzed by, e.g., Panaitescu & Kumar (2002), the conclusion being that at least some bursts may occur in high mass-loss winds, as expected from massive progenitors. The parameters for such wind fits are uncertain because of poorly known stellar mass-loss rates.

In this Letter we show that observations of prompt optical/IR and/or X-ray emission attributable to reverse-shock emission could constrain the GRB environment. In high-density environments, the self-absorption (SA) frequency is much higher than in the normal ISM, and it could be higher than the cooling and the typical injection peak frequencies (Wu et al. 2003). Here we argue that in such situations the SA frequency and its scaling are different from, and the flux at the SA frequency is appreciably larger than, what had been previously estimated. This implies a different light-curve time behavior for the afterglow prompt flash in a dense environment. This is of significant interest, since observations of the SA frequency and the net flux could provide constraints on the otherwise poorly known wind mass-loss rates of progenitor stars or on the presence of a dense ISM. These new features are expected to be pronounced if the inverse Compton (IC) process does not play a dominant role. This could happen in the case of highly magnetized fireball ejecta, whose presence has been suggested by some recent studies (Zhang, Kobayashi, & Mészáros 2003; Kumar & Panaitescu 2003; Coburn & Boggs 2003). The strength of the SA features would then provide a constraint on the magnetization parameter.

[1] Department of Astronomy and Astrophysics, Pennsylvania State University, 525 Davey Laboratory, University Park, PA 16802.
[2] Center for Gravitational Wave Physics, Pennsylvania State University, University Park, PA 16802.
[3] Institute for Advanced Study, Einstein Drive, Princeton, NJ 08540.

2. THE MODEL

We consider a relativistic shell with an isotropic energy E, an initial Lorentz factor η, and an initial width Δ_0 expanding into a surrounding medium with a density distribution $\rho = AR^{-2}$. The shell width Δ_0 is related to the intrinsic duration of the GRB as $\Delta_0 \sim (1+z)^{-1}cT$ (Kobayashi, Piran, & Sari 1997), where z is the redshift of the burst. The evolution of reverse shocks propagating into shells can be classified into two cases depending on the value of the initial bulk Lorentz factor η relative to a critical value $\eta_{\rm cr} = [(1+z)E/4\pi Ac^3T]^{1/4}$ (Sari & Piran 1995; Kobayashi & Zhang 2003b). Most bursts in a wind environment fall in the thick-shell class ($\eta > \eta_{\rm cr}$), because the high density implies a critical Lorentz factor $\eta_{\rm cr} \sim 70\zeta^{1/4}E_{53}^{1/4}A_{11.7}^{-1/4}T_{50}^{-1/4}$ lower than the typical value in fireball models $\eta \gtrsim 100$ (e.g., Lithwick & Sari 2001), where $\zeta = (1+z)/2$, $E_{53} = E/10^{53}$ ergs, the duration $T_{50} = T/50$ s, and $A_{11.7} = A/5 \times 10^{11}$ g cm^{-1} is a typical wind mass-loss rate. We focus on the thick-shell case, for which one can take the shock crossing time $t_\times \sim T$ and the bulk Lorentz factor during the shock crossing ($t < t_\times$) is $\Gamma \sim \eta_{\rm cr}$.

If we neglect SA (which is discussed in the next section), the synchrotron spectrum of the reverse shock is described by a broken power law with a peak $F_{\nu,\,\rm max}$ and two break frequencies: a typical frequency ν_m and a cooling frequency ν_c (Sari, Piran, & Narayan 1998). Assuming that constant fractions (ϵ_e and ϵ_B) of the internal energy produced by the shock go into the electrons and the magnetic field, the reverse-shock spectrum at a shock crossing time $t_\times \sim T$ is characterized by (Kobayashi & Zhang 2003b) $\nu_c(T) \sim 1.5 \times 10^{11}\zeta^{-3/2}\epsilon_{B,-1}^{-3/2}E_{53}^{1/2}A_{11.7}^{-2}T_{50}^{1/2}$ Hz, $\nu_m(T) \sim 5.0 \times 10^{12}\zeta^{-1/2}\epsilon_{e,-2}^{2}\epsilon_{B,-1}^{1/2}E_{53}^{-1/2}A_{11.7}\eta_2^2T_{50}^{-1/2}$ Hz, and $F_{\nu,\,\rm max}(T) \sim 95d^{-2}\zeta^2\epsilon_{B,-1}^{1/2}E_{53}A_{11.7}^{1/2}\eta_2^{-1}T_{50}^{-1}$ Jy, where $\epsilon_{B,-1} = \epsilon_B/10^{-1}$, $\epsilon_{e,-2} = \epsilon_e/10^{-2}$, $\eta_2 = \eta/100$, $d = d_L(z)/(2 \times 10^{28}\ {\rm cm})$, $d_L(z)$ is the luminosity distance of the burst, and $d_L(1) \sim 2 \times 10^{28}$ cm for the standard cosmological parameters ($\Omega_m = 0.3$, $\Omega_\Lambda = 0.7$, and $h = 0.7$). The value of $\epsilon_B(\epsilon_e)$ assumed for the reverse-shock emission is larger (smaller) than in some previous broadband fits of afterglow forward shocks (e.g., Wijers & Galama 1999; Panaitescu & Kumar 2001). However, ϵ_e and ϵ_B can in principle differ in the forward- and reverse-shock regions, and as shown recently, ϵ_B in the reverse shock (fireball ejecta) could be much higher than in the forward shock (Zhang et al. 2003; Kumar & Panaitescu 2003).

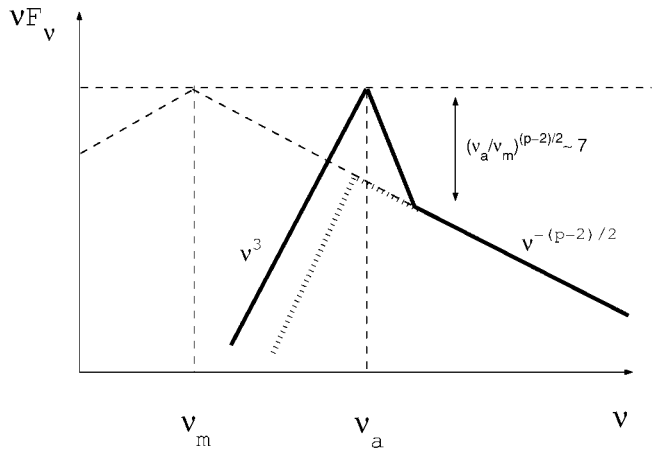

FIG. 1.—Reverse-shock spectrum in a dense environment or wind when synchrotron losses dominate: with SA (*thick solid line*) and without SA (*thin dashed line*). The schematic SA maximum would appear as a rounded thermal peak. The previous self-absorbed flux estimate is shown by hashed lines. The correction factor $2(\nu_a/\nu_c)^{(p-2)/2} \propto t^{(p-2)/7}$ is slightly larger at later times ($t \sim t_\times$); the value of ~7 is evaluated at t_a for typical parameters.

3. SA AND OPTICAL/IR REVERSE FLASH

In a stellar wind the external density at the initial interaction with the shell is much larger than in the typical ISM, hence the cooling frequency ν_c is lower than the typical peak frequency ν_m, and the synchrotron SA frequency ν_a can be much higher than ν_m: $\nu_c(T) < \nu_m(T) < \nu_a(T)$. As suggested by some recent work, the fireball ejecta could be highly magnetized. In such cases the condition $\epsilon_e/\epsilon_B \ll 1$ can lead to a Compton parameter $Y \ll 1$ and the IC process is not important for electron cooling (the opposite case $Y \gg 1$ is discussed below). A consequence of the synchrotron dominance is that SA suppresses the emission below the SA frequency ν_a and prevents the electrons from cooling down to the Lorentz factor γ_c corresponding to the cooling frequency ν_c. The suppressed radiation energy is partly redistributed among the electrons and results in a distinctive hump in the spectrum of the reverse-shock emission.

The reverse shock injects electrons with a power-law energy distribution $N(\gamma)d\gamma \propto \gamma^{-p}d\gamma(\gamma \geq \gamma_m)$. The energy deposited in electrons with Lorentz factors between γ_m and γ_a is $E_e \sim (p-1)N_t\Gamma\gamma_m m_e c^2/(p-2)$, where N_t is the number of electrons in the shell, γ_a is the Lorentz factor corresponding to the SA frequency, and we assumed that $p > 2$ and $\gamma_a \gg \gamma_m$ (so E_e is essentially the total electron energy). This energy is redistributed among the electrons and photons in the optically thick regime on a timescale comparable to the cooling time (Ghisellini & Svensson 1989). Since the reverse shock is in the fast-cooling regime, the electrons have enough time to redistribute the energy. In a dynamical time, the energy E_e is radiated as photons around ν_a. Assuming $p = 3$, the flux at ν_a is given by

$$F_{\nu_a}(T) \sim \frac{1}{4\pi d_L^2}\frac{E_e}{\nu_a T} \sim \frac{2(\nu_c\nu_m)^{1/2}}{\nu_a}F_{\nu,\,\max}. \quad (1)$$

A simple estimate of the maximal SA flux is given by a blackbody flux with the reverse-shock temperature (e.g., Sari & Piran 1999), $F_{\nu_a}^{\rm bb} = 2\pi(1+z)^3\nu_a^2 m_e\Gamma\gamma_a(R_\perp/d_L)^2$, where $R_\perp \sim 2\Gamma cT/(1+z)$ is the observed size of the shell. Equating $F_{\nu_a}^{\rm bb} \sim F_{\nu_a}$, we obtain the SA frequency

$$\nu_a(T) \sim 8.1 \times 10^{13}\zeta^{-3/14}\epsilon_{e,-2}^{2/7}\epsilon_{B,-1}^{1/14}A_{11.7}^{2/7}E_{53}^{1/14}T_{50}^{-11/14}\ {\rm Hz}. \quad (2)$$

An alternative derivation of the SA frequency is obtained by requiring the electron synchrotron cooling rate and heating rate (through absorption) to be equal at γ_a. The cross section for the synchrotron absorption process is approximately $\sigma_s \sim \gamma^{-5}r_e r_{\rm L}$ (e.g., Ghisellini & Svensson 1991), where r_e and $r_{\rm L}$ are the classical electron radius and the Larmor radius, respectively. Using this cross section and the photon flux determined by equation (1), we can evaluate the heating rate, while the cooling rate is given by the electron synchrotron power. Equating these rates reproduces the SA frequency of equation (2).

Following Kobayashi & Zhang (2003b), we obtain the scalings at $t < t_\times$ of the spectral quantities $\nu_c \propto t$, $\nu_m \propto t^{-1}$, $\nu_a \propto t^{-5/7}$, and $F_{\nu,\,\max} \propto t^0$. The optical/IR luminosity initially increases as $\sim(\nu/\nu_a)^2F_{\nu_a} \propto t^{15/7}$. When the SA frequency passes through the observation band $\nu_{\rm obs}$ at t_a, the flux reaches a peak of $F_{\nu_{\rm obs}}(t_a) \sim 2(\nu_m\nu_c)^{1/2}F_{\nu,\,\max}/\nu_{\rm obs}$, and then it rapidly decreases. For electrons in the hump that are quasi-thermally distributed, the flux beyond the peak would decrease proportional to $\exp(-t^{5/7})$ (or, if the emission of the quasi-thermal electrons above the peak is fitted by a power law ν^{-k} above ν_a, the decrease is proportional to $t^{-(5/7)(k-1)}$), the flux dropping by a factor $\mathcal{R} \sim 2[\nu_{\rm obs}/\nu_m(t_a)]^{(p-2)/2}$. The time t_a of the SA frequency passage through the K band, the peak flux $F_{\nu_K}(t_a)$, and the peak flux contrast $\mathcal{R}$ relative to the subsequent power-law decay value are given by

$$t_a \sim 20\zeta^{-3/10}\epsilon_{e,-2}^{2/5}\epsilon_{B,-1}^{1/10}A_{11.7}^{2/5}E_{53}^{1/10}T_{50}^{-1/10}\nu_{\rm obs,\,14.2}^{-7/5}\ {\rm s}, \quad (3)$$

$$F_{\nu_K}(t_a) \sim 1d^{-2}\zeta\epsilon_{e,-2}E_{53}T_{50}^{-1}\nu_{\rm obs,\,14.2}^{-1}\ {\rm Jy}, \quad (4)$$

$$\mathcal{R} \sim 7\zeta^{1/10}\epsilon_{e,-2}^{-4/5}\epsilon_{B,-1}^{-1/5}A_{11.7}^{-3/10}E_{53}^{3/10}\eta_2^{-1}T_{50}^{-3/10}\nu_{\rm obs,\,14.2}^{-1/5}, \quad (5)$$

where $\nu_{\rm obs,\,14.2} = \nu_{\rm obs}/(1.6 \times 10^{14}\ {\rm Hz})$ and $p = 3$ was assumed. At this turnover, a color change from blue to red is expected (see Fig. 1). Since the polarization is zero for an optically thick quasi-thermal spectrum, the reverse-shock shell can emit polarized photons only above the turnover. If a turnover characterized by t_a and $F_{\nu_K}(t_a)$ is observed, we can constrain the mass-loss rate A, assuming that the redshift z is measured and the GRB explosion energy E is determined from late-time afterglow observations. The peak flux determines ϵ_e via equation (4), and the peak time gives through equation (3) a constraint on the mass-loss rate $A \sim 5 \times 10^{11}\epsilon_{B,-1}^{-1/4}\zeta^{3/4}\epsilon_{e,-2}^{-1}E_{53}^{-1/4}T_{50}^{1/4}\nu_{\rm obs,\,14.2}^{7/2}(t_a/20\ {\rm s})^{5/2}$ g cm^{-1}, where the dependence on the parameter ϵ_B is weak.

After the optical/IR reverse-shock emission drops to the level expected from the usual synchrotron model, the flux decreases slowly as $\sim(\nu_m/\nu_c)^{-1/2}(\nu/\nu_m)^{-p/2}F_{\nu,\,\max} \sim t^{-(p-2)/2}$. Beyond a timescale comparable to the burst duration T, the optical/IR emission fades rapidly because no further electrons are shocked in the shell. The angular time delay effect prevents the abrupt disappearance of the reverse component, whose flux decreases steeply as $\sim t^{-(p+4)/2}$ (Kumar & Panaitescu 2000; Kobayashi & Zhang 2003b). No color change is expected around this break. The flux at this break for $p = 3$ is $F_{\nu_K}(T) \sim 0.1d^{-2}\zeta^{3/4}\epsilon_{e,-2}^2\epsilon_{B,-1}^{1/4} \times A_{11.7}^{1/2}E_{53}^{3/4}\eta_2 T_{50}^{-5/4}\nu_{\rm obs,\,14.2}^{-3/2}$ Jy. These two breaks are schematically shown in Figure 2, the break sharpness being an idealization; in reality these would be rounded. In our treatment, we have ignored pair formation ahead of the blast wave, e.g., Beloborodov (2002), which may modify the forward-shock spectrum and light curve.

4. IC EFFECTS AND PROMPT REVERSE X-RAY FLASH

The above discussion assumed magnetized ejecta with $\epsilon_e/\epsilon_B \ll 1$ and $Y < 1$. However, for weaker ejecta magnetization with $\epsilon_e/\epsilon_B \gg 1$, the IC process can affect the observed spectrum

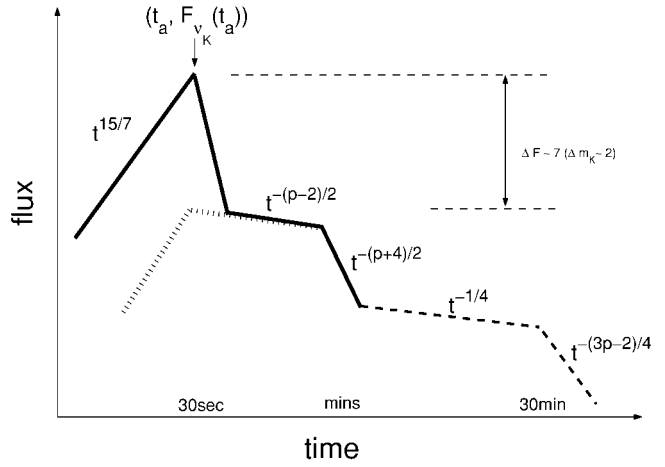

FIG. 2.—Schematic optical light curve for a synchrotron-dominated fireball in a dense environment or wind: reverse-shock emission (*solid line*) and forward-shock emission (*dashed line*). The hashed line shows a previous estimate. Timescales are rough estimates for the typical parameters.

and the light curve, resulting in a reverse-shock prompt X-ray flare. (For forward shocks, the importance of IC emission has been discussed, e.g., by Sari & Esin 2001 and Panaitescu & Kumar 2001). The energy available for the synchrotron process is reduced from the injected energy E_e by a factor of $(1 + Y)$, where $Y \sim (\epsilon_e/\epsilon_B)^{1/2}$ (e.g., Zhang & Mészáros 2001). The IC process enhances the electron cooling, so ν_c is smaller by a factor of $(1 + Y)^2$ than its previous (synchrotron-only) value. The thermal bump is shifted to a lower frequency, becoming less prominent or even disappearing. As a consequence of the IC cooling, the flux at ν_a becomes smaller by a factor of $\sim(1 + Y)$ than the value given by equation (1). If ν_a is shifted below ν_m, most of the energy available for the synchrotron process is radiated between ν_a and ν_m. The flux at ν_a is reduced from equation (1) by a factor of $\sim(1 + Y)(\nu_m/\nu_a)^{1/2}$. By equating the flux at ν_a and the blackbody flux at the reverse-shock characteristic temperature, we can obtain the SA frequency. For the same parameters as for equation (1) but taking $\epsilon_{e,-1} = \epsilon_e/10^{-1}$ and $\epsilon_{B,-3} = \epsilon_B/10^{-3}$, we get $\nu_a(T) \sim 5.8 \times 10^{13}\zeta^{-3/14}\epsilon_{e,-1}^{1/7} \times \epsilon_{B,-3}^{3/14}A_{11.7}^{2/7}E_{53}^{1/14}T_{50}^{-11/14}$ Hz and $\nu_m(T) \sim 5.0 \times 10^{13}\zeta^{-1/2}\epsilon_{e,-1}^{2} \times \epsilon_{B,-3}^{1/2}E_{53}^{-1/2}A_{11.7}\eta_2^2T_{50}^{-1/2}$ Hz. When $\nu_a \lesssim \nu_m$, as in this case, the contrast $\mathcal{R}$ is $\lesssim$2 and the bump practically disappears. The optical/IR light curve initially increases as $\sim(\nu/\nu_a)^{5/2}F_{\nu_a} \propto t^{5/2}$, and after ν_a crosses the observation band, it decreases as $t^{-(p-2)/2}$.

Since at the shock crossing time, the forward- and reverse-shocked regions have roughly comparable energy, the νF_ν peaks of the synchrotron emissions reach roughly similar levels. Assuming that the characteristic reverse-shock IC frequency $\nu_{a,\mathrm{IC}} \sim \gamma_a^2\nu_a$ is close to the typical (peak) frequency of the forward-shock synchrotron emission, we can infer that in the case of $Y \ll 1$ the reverse-shock IC component is generally masked by the forward-shock synchrotron emission, whereas in the case of $Y \gg 1$ the reverse-shock IC peak sticks out above the forward-shock synchrotron peak. Therefore, for weakly magnetized fireballs (with $Y \gtrsim 1$), a prompt X-ray flare is expected from the reverse shock. The characteristic photon energy and the flux at this frequency are $h\nu_{a,\mathrm{IC}}(T) \sim 20\zeta^{-3/7}\epsilon_{e,-1}^{2/7}\epsilon_{B,-3}^{-1/14}E_{53}^{1/7}A_{11.7}^{1/14}T_{50}^{-4/7}$ keV and $F_{\nu_a,\mathrm{IC}}(T) \sim 1d^{-2}\zeta^{31/14}\epsilon_{e,-1}^{9/7}\epsilon_{B,-3}^{3/7}E_{53}^{9/14}A_{11.7}^{15/14}T_{50}^{-17/14}$ mJy, respectively. The typical duration of this X-ray flare at $\nu \gtrsim \nu_{a,\mathrm{IC}}$ is of the order of the shock crossing time $t_\times \sim T = 50T_{50}$ s. After the reverse shock crosses the shell, electrons are no longer heated and the (on-axis) synchrotron flux at $\nu > \nu_a(T)$ drops, as does the the IC emission at $\nu > \nu_{a,\mathrm{IC}}$, and one starts to observe high-latitude emission. The X-ray emission from the reverse shock decays steeply as $t^{-(p+4)/2}$, whereas the forward-shock emission decays proportional to $t^{-(3p-2)/4}$. Thus the slower decaying forward-shock component eventually starts to dominate.

5. DENSE ISM IN EARLY GALAXIES

We consider a specific model in which the ISM density of early galaxies scales with redshift as $n \sim (1 + z)^4 n_0$ cm^{-3} (e.g., Ciardi & Loeb 2000). In this case (or in general when the ISM density is much larger than a typical $n_0 \sim 1$ cm^{-3} at $z = 0$), a discussion analogous to that of the previous section can also lead to a bump in the reverse-shock spectrum and in the optical/IR light curve.

A large fraction of GRBs are expected to be classified as thick shell cases in this model, whose spectral quantities are given by (Kobayashi & Zhang 2003a) $\nu_c(T) \sim 2.0 \times 10^{11}n_0^{-1}\zeta_6^{-9/2} \times \epsilon_{B,-1}^{-3/2}E_{53}^{-1/2}T_{2.2}^{-1/2}$ Hz, $\nu_m(T) \sim 7.2 \times 10^{11}n_0^{1/2}\zeta_6\epsilon_{e,-2}^2\epsilon_{B,-1}^{1/2}\eta_2^2$ Hz, and $F_{\nu,\max}(T) \sim 27n_0^{1/4}D^{-2}\zeta_6^{11/4}\epsilon_{B,-1}^{1/2}E_{53}^{5/4}\eta_2^{-1}T_{2.2}^{-3/4}$ Jy, where $\zeta_6 = (1 + z)/6$, $T_{2.2} = T/150$ s, $D = d_L(z)/(1.5 \times 10^{29}$ cm) is the normalized luminosity distance, and $D(z = 5) = 1$. Equating $F_{\nu_a}^{\mathrm{bb}} \sim F_{\nu_a}$, we obtain $\nu_a(T) \sim 3.7 \times 10^{13}n_0^{1/7}\zeta_6^{3/14}\epsilon_{e,-2}^{2/7}\epsilon_{B,-1}^{1/14} \times E_{53}^{3/14}T_{2.2}^{-9/14}$ Hz. Using the scalings by Kobayashi (2000), one can show that $\nu_a \propto t^{-3/7}$ during the shock crossing. The optical/IR light curve initially increases as $\sim(\nu/\nu_a)^2F_{\nu_a} \propto t^{9/7}$. When ν_a passes through the K band at $t_a \sim 5n_0^{1/3}\zeta_6^{1/2}\epsilon_{e,-2}^{2/3}\epsilon_{B,-1}^{1/6}E_{53}^{1/2}T_{2.2}^{-1/2}\nu_{\mathrm{obs},14.2}^{-7/3}$ s, the flux reaches a peak of $F_{\nu_K}(t_a) \sim 0.1D^{-2}\zeta_6\epsilon_{e,-2}E_{53}T_{2.2}^{-1}\nu_{\mathrm{obs},14.2}^{-1}$ Jy, and then it rapidly decreases by a (bump contrast) factor of $\mathcal{R} \sim 30n_0^{-1/4}\zeta_6^{-1/2}\epsilon_{e,-2}^{-1}\epsilon_{B,-1}^{-1/4}\eta_2^{-1}\nu_{\mathrm{obs},14.2}^{1/2}$ ($p = 3$). After the emission drops to the level expected from the usual synchrotron model, the flux keeps a constant level, and then it rapidly fades as $t^{-(p+4)/2}$ after a time comparable to the burst duration.

6. DISCUSSION AND CONCLUSIONS

We have analyzed the prompt afterglow emission from the reverse shocks of GRBs occurring in dense environments, such as the stellar wind of a massive progenitor or a dense ISM as might be expected in early galaxies. Usually in the fast cooling case, the νF_ν flux is normalized at the typical frequency ν_m by using the energy ejected into electrons. However, here we point out that if the synchrotron SA frequency ν_a is higher than the typical frequency ν_m (and ν_c), this usual prescription should be inapplicable for estimating the flux at and below ν_a. Such conditions can occur in the reverse shock of a GRB fireball in a dense environment. The radiation flux suppressed by the SA effect is redistributed among the electrons and photons in the optically thick regime, and most of it is emitted at $\sim\nu_a$ in a dynamical time. As a result, the SA frequency is different and scales differently with the shock parameters, and the flux at the SA frequency shows a bump that is a factor of $2(\nu_a/\nu_m)^{(p-2)/2}$ (approximately several) above the usual power-law flux estimate for typical parameters. The flux well above ν_a is the same as before, but the flux below ν_a is larger by the same factor $2(\nu_a/\nu_m)^{(p-2)/2}$. This results in a new type of temporal behavior for the prompt optical flash of afterglows from fireballs in dense (e.g., wind or early galaxy) environments. These new features will be prominent when the IC process is not important for electron cooling, i.e., for ejecta with $\epsilon_e/\epsilon_B \ll 1$. This may be the case in fireball ejecta that are highly magnetized, as suggested by some recent studies. If, on the other hand, the burst occurs in a dense environment and such features are absent, this may be an indication that $\epsilon_e/\epsilon_B \gg 1$, and in this case a prompt reverse-shock X-ray flare is expected.

Massive stars appear implicated in producing long GRBs (e.g., Stanek et al. 2003). Wind mass loss is expected from

such stars previous to the GRB explosion, but snapshot fits to forward-shock late emission (e.g., Panaitescu & Kumar 2002) are compatible with such wind mass loss in only a handful of cases. In general the parameters of stellar winds are poorly known, and the uncertainties are further increased at high redshifts, where massive stars are expected to be metal-poor. For this reason, signatures of a wind mass loss or a dense environment would be extremely valuable, both for GRB astrophysics and for tracing the properties of star formation at high redshifts. The prompt optical flashes expected after tens of seconds from the reverse shock in a dense environment would give characteristic signatures in the spectral and temporal behavior. These may help us to test for the presence of winds and constrain the wind mass loss, in moderate-redshift environment, or alternatively, at high redshifts they may provide evidence for a denser ISM than at low redshifts. In such winds or dense ISM the spectra and light-curve time behavior can also give constraints on the strength of the magnetic field in the ejecta. Large numbers of prompt X-ray detections with future missions such as *Swift*, complemented by ground-based follow-ups, should be able to test for such wind or dense ISM signatures and trace any changes with redshifts, if they exist, thus constraining the GRB environment as well as the radiation mechanisms.

We thank M. J. Rees, J. Granot, A. Beloborodov, and the referee for valuable comments. This work is supported by NASA NAG5-13286, NSF AST 00-98416, the Monell Foundation, and the Pennsylvania State University Center for Gravitational Wave Physics, funded under cooperative agreement by NSF PHY 01-14375.

REFERENCES

Beloborodov, A. M. 2002, ApJ, 565, 808
Chevalier, R. A., & Li, Z. Y. 1999, ApJ, 520, L29
———. 2000, ApJ, 536, 195
Ciardi, B., & Loeb, A. 2000, ApJ, 540, 687
Coburn, W., & Boggs, S. E. 2003, Nature, 423, 415
Frail, D. A., et al. 2001, ApJ, 562, L55
Ghisellini, G., & Svensson, R. 1989, in Physical Processes in Hot Cosmic Plasmas, ed. W. Brinkmann, A. C. Fabian, & F. Giovannelli (Dordrecht: Kluwer), 395
———. 1991, MNRAS, 252, 313
Kobayashi, S. 2000, ApJ, 545, 807
Kobayashi, S., Piran, T., & Sari, R. 1997, ApJ, 490, 92
Kobayashi, S., & Zhang, B. 2003a, ApJ, 582, L75
———. 2003b, ApJ, 597, 455
Kumar, P., & Panaitescu, A. 2000, ApJ, 541, L51
Kumar, P., & Panaitescu, A. 2003, MNRAS, 346, 905
Li, Z. Y., & Chevalier, R. A. 2003, ApJ, 589, L69
Lithwick, Y., & Sari, R. 2001, ApJ, 555, 540
Panaitescu, A., & Kumar, P. 2001, ApJ, 560, L49
———. 2002, ApJ, 571, 779
Sari, R., & Esin, A. A. 2001, ApJ, 548, 787
Sari, R., & Piran, T. 1995, ApJ, 455, L143
———. 1999, ApJ, 517, L109
Sari, R., Piran, T., & Narayan, R. 1998, ApJ, 497, L17
Stanek, K. Z., et al. 2003, ApJ, 591, L17
Wijers, R. A. M. J., & Galama, T. J. 1999, ApJ, 523, 177
Wu, X. F., et al. 2003, MNRAS, 342, 1131
Zhang, B., Kobayashi, S., & Mészáros, P. 2003, ApJ, 595, 950
Zhang, B., & Mészáros, P. 2001, ApJ, 559, 110